Published in final edited form as:
Diabetologia. 2010 July ; 53(7): 1438–1450. doi:10.1007/s00125-010-1696-x.

Deficiency of *ATF3*, an adaptive-response gene, protects islets and ameliorates inflammation in a syngeneic transplantation model

E. J. Zmuda[1,2,3], **M. Viapiano**[1,3,4], **S. T. Grey**[6], **G. Hadley**[5], **A. Garcia-Ocaña**[7], and **T. Hai**[1,2,3,8]

[1]Molecular, Cellular and Developmental Biology Program, Ohio State University, Columbus, OH 43210, USA

[2]Department of Molecular and Cellular Biochemistry, Ohio State University, Columbus, OH 43210, USA

[3]Center for Molecular Neurobiology, Ohio State University, Columbus, OH 43210, USA

[4]Department of Neurological Surgery, Ohio State University, Columbus, OH 43210, USA

[5]Department of Surgery, Ohio State University, Columbus, OH 43210, USA

[6]Gene Therapy and Autoimmunity Group, Garvan Institute of Medical Research, Darlinghurst, NSW 2010, Australia

[7]Department of Medicine, Division of Endocrinology and Metabolism, and Department of Cell Biology and Physiology, University of Pittsburgh, Pittsburgh, PA 15261, USA

Abstract

Aims/hypothesis—Islet transplantation is a potential therapeutic option for type 1 diabetes. However, the need for multiple donors per patient and heavy immunosuppression of the recipients limit its use. The goal of this study was to test whether *Activating Transcription Factor 3* (*ATF3*), a stress-inducible pro-apoptotic gene, plays a role in graft rejection in islet transplantation.

Methods—We compared wild type (WT) and *ATF3* knockout (KO) islets in vitro using stress paradigms relevant to islet transplantation: isolation, inflammation, and hypoxia. We also compared the WT and KO islets in vivo using a syngeneic mouse transplantation model.

Results—*ATF3* was induced in all three stress paradigms and played a deleterious role in islet survival, as evidenced by the lower viability of WT islets than KO islets. ATF3 up-regulated various downstream target genes in a stress-dependent manner. These target genes can be classified into two functional groups: (a) apoptosis (*Noxa*, *bNIP3*), and (b) immuno-modulation (*TNFα*, *IL-1β*, *IL-6*, and *CCL2/MCP-1*). In vivo, *ATF3* KO islets performed better than WT islets after transplantation, as evidenced by better glucose homeostasis in the recipients and the reduction of the following parameters in the KO grafts: caspase 3 activation, macrophage infiltration, and expression of the above apoptotic and immuno-modulatory genes.

Conclusions/interpretation—*ATF3* plays a role in islet graft rejection by contributing to islet cell death and inflammatory responses at the graft sites. Silencing *ATF3* may provide therapeutic benefits in islet transplantation.

[8]Corresponding author: T. Hai, Room 174 Rightmire Hall, 1060 Carmack Road, Ohio State University, Columbus, OH 43210; Fax: (614) 292-5379; Tel: (614) 292-2910; hai.2@osu.edu.

Duality of interest The authors declare that there is no duality of interest associated with this manuscript.

Keywords

islet transplantation; primary non-function; stress response; transcription factor; inflammation; cell death, *ATF3*

Introduction

Since the pioneering work demonstrating that transplantation of islets of Langerhans into diabetic rodents could normalize their blood glucose levels, islet transplantation has been proposed to be a potential treatment for type 1 diabetes [1–7]. Recent advances in human islet transplantation [1,8] further strengthened this view. However, major limitations prevent islet transplantation from becoming a widespread clinical reality: (a) the requirement for large numbers of islets per patient severely reduces the number of potential recipients, and (b) the need for heavy immunosuppression significantly affects the pediatric population of patients due to their vulnerability to long-term immunosuppression. Strategies that can overcome these limitations will greatly enhance the therapeutic potential of islet transplantation.

A major reason for islet loss during transplantation is the apoptotic death of islet cells, an event caused by multiple factors that can be classified into two main groups. The first consists of those leading to “primary non-function,” a term referring to islet dysfunction and loss due to reasons other than specific immune rejection by the recipients. Factors causing primary non-function include deleterious conditions that islets face during isolation and the hostile environment in the recipients such as the hyperglycemic milieu of the hosts and the non-specific inflammatory attack by the host innate-immunity, which involves macrophages and dendritic cells [9–17]. The second group of factors causing islet death in transplantation is the specific immune attacks by the host adaptive-immunity, which involves T and B lymphocytes.

Although both primary non-function and specific immune attack contribute to graft failure, primary non-function is thought to be the main reason for islet failure in the early transplantation stage and for the requirement of a large number of islets (≥2 pancreata/patient) to achieve euglycemia (see [18] for references). Despite its importance, primary non-function is not well understood at the molecular level. In this study, we investigated the potential roles of *Activating Transcription Factor 3* (*ATF3*), a stress-inducible pro-apoptotic gene, in primary non-function. *ATF3* encodes a member of the ATF/CREB family of transcription factors that share the basic region/leucine zipper DNA binding motif and bind to the ATF/CRE consensus sequence TGACGTCA (some reviews, [19,20]). Overwhelming evidence indicates that the expression of *ATF3* is up-regulated by a variety of signals, including some seemingly unrelated signals such as cytokines, nutrient depravation, serum stimulation, and calcium signaling (a review, [21]). Given the broad spectrum of the stimuli that can induce *ATF3*, it appears that *ATF3* is an “adaptive-response” gene used by the cells to adapt to extra- and/or intra-cellular changes. Borrowing a concept from the network theory, we suggest that *ATF3* can be viewed as a hub in the biological networks to respond to signals perturbing homeostasis. Functionally, *ATF3* is pro-apoptotic in pancreatic beta cells. Previously, we demonstrated that knockout or knockdown of *ATF3* protects islets or beta cells from stress-induced death [22,23].

The deleterious effect of *ATF3* in beta cells, combined with its general inducibility, prompted us to hypothesize that *ATF3* is induced by signals encountered by the islets during transplantation, and that deletion of *ATF3* would protect islets in a syngeneic transplantation model. In this model, donor mice have the same genetic background as recipient mice; thus the islets would not invoke the adaptive-immune response, allowing us to investigate the roles of *ATF3* in primary non-function. In this report, we present evidence supporting our hypothesis. We also present evidence that ATF3 up-regulates the expression of several pro-inflammatory

cytokines and *CCL2* (*MCP-1*), which encodes a potent macrophage recruitment factor [24]. These results suggest that *ATF3* contributes to not only apoptosis but also an inflamed state of the islet grafts. Considering the deleterious effects of apoptosis and inflammation, our findings have significant implications for islet transplantation.

Methods

Cell culture and treatments

INS-1 and INS-r3 cells were grown as previously [25]. Treatments were the following: IL-1β (5ng/ml), TNFα (30ng/ml), IFNγ (125ng/ml), and hypoxia (1% O_2, 5% CO_2, 94% N_2).

Animals and adenoviruses

Wt and *ATF3* KO mice were detailed previously [22]. Animal experiments followed the guidelines (NIH publication no. 85-23) and were approved by the Ohio State University Laboratory Animal Resources. Adenoviruses were described previously [23].

Islet isolation and transplantation

Islets isolated from age-matched male mice (12–20 weeks, C57BL/6 background) as previously [23] were incubated with RPMI containing 10% fetal bovine serum (250 islets in 3ml). Transplantations beneath the kidney capsule were carried out as previously [26,27] using 250–400 (as specified) freshly isolated islets.

Graft recovery

Two days after transplantation, the graft was excised, placed into Trizol, vortexed (2 minutes), and rocked (overnight, 4°C) prior to RNA extraction. For controls, similar sized kidney capsules were excised from mice transplanted with PBS.

qRT-PCR, ChIP, immunoblot, and immunohistochemistry

All procedures were according to [23,28], using PCR primers and antibodies listed in the Supplemental.

Cell viability analysis

Islets were stained with propidium iodide (1 μg/ml) and Hoechst 33258 (2μg/ml) followed by epifluorescence analyses using the NIH ImageJ Software as detailed in Supplemental Fig. 1.

Cell fractionation

INS cells were permeabilized with 0.025% digitonin buffer (20mM Hepes, pH7.5, 100mM KCl, 2.5mM $MgCl_2$, 250mM sucrose) on ice for 20 minutes, tested by trypan blue to verify permeability, and spun (12,000×g, 20 minutes) to obtain the cytosolic fraction (supernatant).

Glucose tolerance tests and insulin ELISA

Glucose tolerance test was described previously [23] and insulin was measured by radioimmunoassay (Linco, St. Charles, MO, USA) using retro-orbital blood.

Boyden chamber macrophage migration assay

Bone marrow cells were isolated from the tibia and differentiated into macrophages as before [29]. Islet conditioned medium was made by incubating 200 islets in 0.5 ml medium for 48 hours. Cell migration assay was carried out as previously [30] using 8×10^5 macrophages.

Semi-quantitation of immunohistochemistry signals

For caspase 3 activation, the NIH ImageJ program was used as follows: (a) delineate the islets —region of interest (ROI)—using the custom-written macro (Supplemental Method); (b) threshold the image and convert to black and white; (c) count the positive pixels; (d) calculate the ratio of the signal pixels to the total pixels in the ROI. For macrophage recruitment, the ROI is the area within the kidney sub-capsule that is not occupied by islets (an example, Supplemental Fig. 4).

Statistics

All quantitative data are expressed as means±SEM, and comparisons made by the Student's *t* test unless otherwise indicated.

Results

The effects of ATF3 KO in islet isolation stress

We examined whether *ATF3* is expressed in the islets after isolation. Fig. 1a shows that the level of *ATF3* mRNA was the highest immediately after isolation and declined at 12–24 hours. Fig. 1b is a representative immunoblot, confirming the induction of *ATF3* in the WT but not KO islets. To test the potential significance of *ATF3* expression, we compared WT and KO islets for their viability using propidium iodide (PI) coupled with Hoechst stain. Viable cells are not permeable to PI and will only be stained by Hoechst; however, dead cells will be stained by both PI and Hoechst. Fig. 1c shows a representative picture with more PI stain in the WT than in the KO islets, indicating that *ATF3* enhances cell death. Data quantification using the NIH ImageJ program (detailed in Supplemental Fig. 1) showed higher percentage of PI-positive pixels in the WT than in the KO islets (Fig. 1d). Interestingly, both the WT and KO islets showed decline in cell death over time, but the WT islets showed a slight rebound at the 48-hour time point, paralleling an increase in *ATF3* expression at this time point.

Since ATF3 is a transcription factor, it must exert its action, at least in part, by regulating downstream genes. We thus examined the expression of various candidate genes by qRT-PCR. We focused on two categories of genes: pro-apoptotic genes and genes involved in immuno-modulation. The reason for testing immuno-modulating genes is that, upon transplantation, the grafts induce immune responses from the hosts. Their ability to modulate the host responses greatly impacts the survival of the grafts. Although limited in scope, our screen showed higher expression of the following genes in the WT than in the KO islets (Fig. 1e): *Noxa*, *bNIP3* (pro-apoptotic genes), and *TNFα*, *IL-1*β, *IL-6*, and *CCL2* (immuno-modulating genes). The differences were statistically significant ($p<0.05$) except for *bNIP3* and *CCL2*, which showed a consistent trend in three independent experiments but the p value was >0.05 (0.13 for bNIP and 0.08 for CCL2). We also examined *CSF-1* (*M-CSF*), a macrophage recruitment factor, and *Tissue Factor* (*TF*), a factor whose expression contributes to islet loss in transplantation [31]. No difference in *CSF-1* expression was observed between the WT and KO islets (Fig. 1e), and the difference for *TF* was subtle (1.6 fold higher in WT, $p<0.03$). These results indicate that ATF3 contributes to the increased expression of certain pro-apoptotic and pro-inflammatory genes and would thus enhance islet apoptosis and inflammation. The notion of increased apoptosis is consistent with the higher cell death in the WT islets shown above (panel c). The functional consequences of *ATF3* in inflammation will be addressed below (Fig. 9).

The effects of ATF3 KO in islet proinflammatory stress

Upon transplantation, grafts face a barrage of attacks from the hosts. We examined the induction of *ATF3* by proinflammatory cytokines, either as a combination of two cytokines (IL-1β+IFNγ) or three cytokines (IL-1β+IFNγ+TNFα). Islets were used 72 hours after

isolation, so that ATF3 levels in the WT islets were relatively low before induction. Fig. 2 shows that *ATF3* was induced by cytokines in the islets both at the mRNA (panel a) and protein (panel b) levels. Previously, we reported that *ATF3* KO islets are partially protected from two cytokine–induced apoptosis as evidenced by the decrease in the cell population with sub-2N DNA content [22]. Consistent with the previous results, *ATF3* KO islets had reduced levels of activated caspase 3 compared to WT islets (Fig. 2b). We then examined the expression of the candidate target genes described above. Fig. 2c shows that the WT islets had higher expression of *TNFα*, *IL-1β*, *IL-6*, and *CCL2* than the KO islets ($p<0.05$), indicating that ATF3 also up-regulates these genes (directly or indirectly) in the islets under the proinflammatory stress. No differences were observed for *bNIP3* or *TF* (Fig. 2c and data not shown). The data for *Noxa* were not reproducible in four repeated experiments (not shown). Since *ATF3* is induced by the proinflammatory cytokines (TNFα, IL-1β), its ability to induce the expression of *TNFα* and *IL-1β* indicates a positive feedback loop.

The effects of ATF3 KO in islet hypoxia stress

Upon removal from the donors, the islets are subjected to hypoxic stress until graft vascularization in the host. We therefore examined the induction of *ATF3* by hypoxia (1% O2). Again, islets at 72 hours after isolation were used to reduce the basal ATF3 level. Because the majority of islets started to disintegrate after four to six hours under hypoxia, it was not possible to keep them continuously under this condition. We found that cyclic exposures of islets to hypoxia (1%) and normoxia (20%) for one hour each allow them to maintain overall integrity for eight hours. At the end of four cycles, the islets start to lose their smooth boarders and appear unhealthy. We therefore terminated the experiments after four cycles of hypoxia and normoxia (Fig. 3a diagram). Immunoblot indicated that *ATF3* was induced at the end of all cycles, and Fig. 3b shows the data for cycles two and four. We also examined the induction of *HIF-1α* as a positive control for the hypoxic conditions (Fig. 3b). PI coupled with Hoechst stain indicated reducing viability (more PI stain) over cycles of hypoxia and normoxia (Fig. 3c). As shown in the representative images, PI signals were always at the center of the islets, consistent with the notion that the center of the islets have least oxygen and are most vulnerable to hypoxic stress. This is in contrast to isolation stress, where PI signals started as scattered on the islet surface then focused in the center of the islets (Fig. 1c), presumably due to the development of a hypoxic center over time. We also quantified the signals by counting PI-positive pixels. Under hypoxia, the size of the islet affects the size of the hypoxic center; the bigger the islets, the bigger the hypoxic center. Thus, we plotted the number of PI-positive pixels against islet size (as measured by Hoechst stain). Fig. 3d shows a bar graph of the PI-positive signals after arbitrarily dividing the islets into four groups: from small (<20,000 Hoechst-positive pixels) to big (>40,000 pixels). After two cycles of hypoxia treatment (top panel), the differences between WT and KO islets were statistically significant in the larger islet groups, and after four cycles (bottom panel), the differences were significant for all four groups. Thus, WT islets were more vulnerable to hypoxic stress than KO islets. We then examined the expression of various candidate genes in the islets after hypoxia stress. To our surprise, no genes showed statistically significant differences between WT and KO islets (Fig. 3e). Thus, under the hypoxia stress, *ATF3* contributes to the reduced viability of the islets via a mechanism independent of the genes we have examined thus far.

The effects of ATF3 knockdown in beta cells

Since the KO mice may develop compensation or adaptation that could complicate the phenotypes, we complemented the KO approach by knockdown. As shown in Fig. 4a and 4b, ATF3 was induced by cytokines in the INS-r3 beta cells and knocking it down reduced cytokine-induced caspase 3 activation. This result indicates that ATF3 promotes cytokine-induced beta cell apoptosis and is consistent with the above data using islets. As a step toward understanding the mechanisms of ATF3 action, we examined the effects of ATF3 knockdown

on cytochrome c release, a key step in apoptosis. Fig. 4c shows that cytokine treatment induced cytochrome c release and ATF3 knockdown reduced it.

Recruitment of ATF3 to the target promoters in the pancreatic beta cells

Taken together, the above results indicate that *ATF3* up-regulates various target genes in a stress-dependent manner and contributes to the lower islet viability under all stresses examined. To address whether ATF3 directly regulates the target genes we reported here, we analyzed their corresponding promoters by several programs and found multiple potential ATF3 binding sites on the promoters (Supplemental Fig. 2). Significantly, the majority of these sites are conserved in mouse and rat. To check the ability of ATF3 to bind to these sites in vivo, we carried out chromatin immunoprecipitation (ChIP) assay using INS-1 and INS-r3 cells infected with adenovirus expressing *ATF3* or β*gal* as a control. Comparable results were obtained from these two cell lines and the data from INS-1 cells are shown in Fig. 5. ATF3 indeed bound to the *Noxa*, *bNIP3*, *IL-1*β, *IL-6*, *CCL2* and *TNF*α promoters. Several controls were carried out for the ChIP assay. (a) The binding of ATF3 to the α- or β-*actin* promoter, which lacks recognizable ATF/CRE sites, was examined. No binding was observed, suggesting (albeit not proving) that the signals we observed on the target genes were not due to non-specific binding. In the same samples, PolII was found to bind to the promoter of β-*actin* (a beta-cell gene) but not α-actin (a non-beta-cell gene), further validating the ChIP procedure (data not shown). (b) For all experiments, the ChIP signals were normalized against the input chromatin and the normalized signals from ATF3-expressing cells were divided by that from βgal-expressing cells to obtain the fold enrichment. If the fold enrichment was the same for the ATF3 antibody and IgG (such as that at the −4,800 site on the *IL-1*β promoter), we interpreted it as background fold enrichment (thus no binding). Only if the fold enrichment using the ATF3 antibody was larger than that using IgG, did we interpret it as ATF3 binding. Supplemental Fig. 2 describes the arbitrary definition of low, medium, and high binding. As summarized in Supplemental Fig. 2 and Table 1, ATF3 bound to various sites on these promoters. We then asked whether the endogenous ATF3 binds to the promoters. We treated the INS-r3 cells with cytokines to increase the levels of ATF3 and examined its binding by ChIP. Fig. 6a shows that ATF3 bound to the indicated sites of these promoters. We note that the binding of endogenous ATF3 was lower than that of the ectopically expressed ATF3 (using the above definition of binding), presumably due to the lower levels of endogenous ATF3. We also examined the binding of the endogenous ATF3 to these promoters in islets. We treated the WT islets with cytokines immediately after isolation to increase ATF3 levels. Fig. 6b shows that ATF3 bound to these promoters, as evidenced by the higher ChIP signals using the ATF3 antibody than IgG. As a control, the *ATF3* KO islets were used. No binding was observed except for IL-6, where some background binding was observed. Collectively, all the above ChIP results indicate that ATF3 binds (directly or indirectly) to the promoters examined.

The roles of ATF3 in a syngeneic islet transplantation model

To test whether *ATF3* KO islets would perform better than WT islets in transplantation, we implanted the islets under the kidney capsules of syngeneic WT mice. Mice were rendered diabetic by streptozotocin one week prior to transplantation. At a saturating dose (400 islets), both WT and KO islets restored euglycemic (Supplemental Fig. 3). At a marginal dose (250 islets), KO islets performed better than the WT islets as indicated by several criteria: (a) lower blood glucose levels from post-operative day (POD) 1 to POD28 (Fig. 7a), (b) higher percent of euglycemic mice from POD 1 to POD28 (Fig. 7b), (c) better glucose tolerance test on POD28 (Fig. 7c), (d) smaller “area under the curve” in the glucose tolerance test (Fig. 7d), and (e) higher serum insulin level on POD28 (Fig. 7e). Removing the grafts at POD28 rendered the mice hyperglycemic (Fig. 7a), confirming that the therapeutic effects were due to the transplanted islets. Since *ATF3* is pro-apoptotic, we examined whether the KO islets had reduced apoptosis using activated caspase 3 as a marker by immunohistochemistry assay. The

signals on POD5 were the highest among the days we examined (POD1, 3, 5, and 7). Semi-quantitation of the signals using the NIH ImageJ program (see Methods) showed that KO islets had a lower percentage of area stained positive for activated caspase 3 than the WT islets (4.51 ±1.07 % versus 15.69±3.12 % in WT, multiple sections from four mice per group, $p<0.05$). Fig. 7f shows some representative images. Parallel experiments using IgG as a negative control showed no signals. We also stained the graft sections for ATF3 and confirmed its expression in the WT but not KO islets. Insulin stain and hematoxylin plus eosin (H&E) stain were shown for comparison.

To examine whether ATF3 contributes to the induction of the pro-apoptotic and pro-inflammatory genes described above, we recovered the grafts and analyzed their mRNAs by qRT-PCR. Consistent with the in vitro data, WT islets had higher expression of *Noxa*, *TNFα*, *IL-1β*, *IL-6*, and *CCL2* than the KO islets (Fig. 8, $p<0.05$), indicating that ATF3 contributes to their up-regulation (directly or indirectly) in the grafts. Since CCL2 is a potent macrophage recruitment factor [24], we asked whether the WT and KO islets differ in their abilities to recruit macrophages by assaying the grafts for F4/80, a macrophage marker [32]. Fig. 9a shows that macrophages were recruited to the grafts starting POD2. Interestingly, they surrounded the grafts without infiltrating them. The recruitment continued to increase over time to POD7, when the experiments were terminated. To semi-quantify the signals, we used the NIH ImageJ program as detailed in the Methods. Fig. 9b shows that macrophage recruitment was lower in the KO than in the WT grafts. Although the difference was only 10–20%, they were statistically significant ($p<0.05$), suggesting that *ATF3* expression in the WT islets contributes to their ability to recruit macrophages. To further test this idea, we compared the ability of the conditioned media derived from WT or KO islets (following the isolation stress) to enhance the motility of macrophages using the Boyden chamber migration assay. We isolated bone marrow cells from the tibia and differentiated them into macrophages in vitro. We then placed the macrophages in the top half of the Boyden chamber and put the conditioned media from the islets in the bottom half, followed by measuring the macrophages on the underside of the membrane at 12 hours after incubation. Normal media was used as a control and macrophage migration under this condition was arbitrarily defined as 1. Fig. 9c shows that conditioned media from the WT islets induced macrophages to migrate more efficiently than that from the KO islets. Thus, the in vitro migration assay supported the notion that ATF3 facilitates macrophage recruitment by the islets.

Discussion

In this report, we present evidence that ATF3 up-regulates pro-apoptotic genes and genes involved in immuno-modulation. Previously, we showed that ATF3 down-regulates *IRS2* [23], a potent pro-survival factor in beta cells, providing a mechanistic insight to the pro-apoptotic action of *ATF3* in pancreatic beta cells [22,23]. Results described in this report indicate that ATF3 up-regulates the expression of *Noxa*, providing another potential explanation for the ability of *ATF3* to promote beta cell death. Since apoptosis is a major reason for islet loss during transplantation, it is not surprising that the *ATF3* KO islets performed better than WT islets in transplantation. Our results are consistent with previous reports that dampening apoptosis improves transplantation. However, our studies differ from previous reports in two key aspects. First, we dampened cell death by deleting a pro-apoptotic gene, rather than ectopically expressing anti-apoptotic genes, such as *A20*, *hepatocyte growth factor*, *Bcl-2*, *Akt*, *IRS2*, and *XIAP* [26,27,33–37]. Since *ATF3* is induced during the course of transplantation, our approach attenuates a naturally occurring deleterious event. Second, ATF3 deficiency also dampens inflammation, a benefit that has not been demonstrated by the other approaches. Since inflammatory response has emerged as an important factor in islet graft rejection (below), this is a significant advantage.

The up-regulation of *CCL2* by ATF3 has important implications. *CCL2* is a chemokine and recruits macrophages [24]. Thus, its up-regulation by ATF3 provides an explanation for the reduced macrophage recruitment in the KO grafts. Functionally, macrophage depletion in the recipients has been demonstrated to improve islet graft survival [16,38]. These results complement and further strengthen the idea that *ATF3* deficiency is beneficial to the islet grafts. The up-regulation of *TNFα*, *IL-1β*, and *IL-6* by ATF3 also has significant implications. These cytokines have been demonstrated to have deleterious effects on beta cells [39,40] and contribute to primary non-function in islet transplantation [18,41]. Since *ATF3* itself is induced in the islets by TNFα and IL-1β, it forms a positive-feedback loop to amplify these pro-inflammatory signals. The relevance of TNFα in human islet transplantation is demonstrated by a clinical trial, where the TNFα receptor antagonist, in conjunction with a glucagon-like peptide-1 agonist, improved the Edmonton Protocol [8]. Thus, the ability of *ATF3* to amplify TNFα signal is of significance. We note that ATF3 has been shown to down-regulate the expression of *TNFα*, *IL-6*, and *IL-12a* in macrophages upon lipopolysaccharide treatment [29,42,43]. Thus, ATF3 functions in macrophages to dampen, rather than enhance, the inflammatory responses (as shown here in islets). Explanations for this apparent discrepancy include the differences in cell types and stress signals.

Taken together, our results suggest a critical role for *ATF3* in primary non-function. To our knowledge, this is the first to demonstrate the protective effects of *ATF3* knockout in islet transplantation, and the first to implicate *ATF3* in the ability of islet grafts to induce inflammatory reactions. In light of the emerging views that inflammation plays an important role in islet graft rejection [44,45], our results suggest that *ATF3* may be a therapeutic target to improve islet transplantation. The benefits of silencing *ATF3* include not only the reduction of intracellular decision to undergo cell death, but also the reduction of the ability of islets to provoke host inflammatory response.

Supplementary Material

Refer to Web version on PubMed Central for supplementary material.

Abbreviations

ATF3	Activating transcription factor 3
bNIP3	BCL2/adenovirus E1B 19kDa interacting protein 3
CCL2/MCP-1	Chemokine (C-C motif) ligand 2/Monocyte chemoattractant protein-1
IL-1β	Interleukin 1 beta
IL-6	Interleukin 6
KO	Knockout
Noxa	Phorbol-12-myristate-13-acetate-induced protein 1
POD	Post-operative day
STZ	Streptozotocin
TNFα	Tumor necrosis factor alpha
WT	Wild type

Acknowledgments

We thank Dr. Lei Zhang for tips on kidney capsule injection and the OSU Veterinary Medicine Histology Core for sectioning islet grafts. The work is supported in part by RO1 DK064938 (to T.H.) and Ohio State Neuroscience Center Core grant (P30-NS045758) from National Institute of Health.

References

1. Shapiro AM, Lakey JR, Ryan EA, et al. Islet transplantation in seven patients with type 1 diabetes mellitus using a glucocorticoid-free immunosuppressive regimen. N. Engl. J. Med 2000;343:230–238. [PubMed: 10911004]
2. Weir GC, Bonner-Weir S. Islet transplantation as a treatment for diabetes. J. Am. Optom. Assoc 1998;69:727–732. [PubMed: 9844324]
3. Hogan A, Pileggi A, Ricordi C. Transplantation: current developments and future directions; the future of clinical islet transplantation as a cure for diabetes. Front. Biosci 2008;13:1192–1205. [PubMed: 17981623]
4. Merani S, Shapiro AM. Current status of pancreatic islet transplantation. Clin. Sci. (Lond) 2006;110:611–625. [PubMed: 16689680]
5. Rother KI, Harlan DM. Challenges facing islet transplantation for the treatment of type 1 diabetes mellitus. J. Clin. Invest 2004;114:877–883. [PubMed: 15467822]
6. Witkowski P, Herold K. Islet transplantation for type 1 diabetes--where should we go? Nat. Clin. Pract. Endocrinol. Metab 2007;3:2–3. [PubMed: 17179921]
7. Naftanel MA, Harlan DM. Pancreatic islet transplantation. PLoS Med 2004;1:e58. [PubMed: 15630467]
8. Gangemi A, Salehi P, Hatipoglu B, et al. Islet transplantation for brittle type 1 diabetes: the UIC protocol. Am. J. Transplant 2008;8:1250–1261. [PubMed: 18444920]
9. Jansson L, Carlsson PO. Graft vascular function after transplantation of pancreatic islets. Diabetologia 2002;45:749–763. [PubMed: 12107718]
10. Davalli AM, Scaglia L, Zangen DH, Hollister J, Bonner-Weir S, Weir GC. Vulnerability of islets in the immediate posttransplantation period. Dynamic changes in structure and function. Diabetes 1996;45:1161–1167. [PubMed: 8772716]
11. Davalli AM, Scaglia L, Zangen DH, Hollister J, Bonner-Weir S, Weir GC. Early changes in syngeneic islet grafts: effect of recipient's metabolic control on graft outcome. Transplant Proc 1995;27:3238–3239. [PubMed: 8539932]
12. Davalli AM, Ogawa Y, Ricordi C, Scharp DW, Bonner-Weir S, Weir GC. A selective decrease in the beta cell mass of human islets transplanted into diabetic nude mice. Transplantation 1995;59:817–820. [PubMed: 7701574]
13. Davalli AM, Ogawa Y, Scaglia L, et al. Function, mass, and replication of porcine and rat islets transplanted into diabetic nude mice. Diabetes 1995;44:104–111. [PubMed: 7813803]
14. Jonas JC, Sharma A, Hasenkamp W, et al. Chronic hyperglycemia triggers loss of pancreatic beta cell differentiation in an animal model of diabetes. J. Biol. Chem 1999;274:14112–14121. [PubMed: 10318828]
15. Montana E, Bonner-Weir S, Weir GC. Beta cell replication and mass in islet transplantation. Adv. Exp. Med. Biol 1997;426:421–427. [PubMed: 9580368]
16. Bottino R, Fernandez LA, Ricordi C, et al. Transplantation of allogeneic islets of Langerhans in the rat liver: effects of macrophage depletion on graft survival and microenvironment activation. Diabetes 1998;47:316–323. [PubMed: 9519734]
17. Biarnes M, Montolio M, Nacher V, Raurell M, Soler J, Montanya E. Beta-cell death and mass in syngeneically transplanted islets exposed to short- and long-term hyperglycemia. Diabetes 2002;51:66–72. [PubMed: 11756324]
18. Wu Y, Han B, Luo H, et al. DcR3/TR6 effectively prevents islet primary nonfunction after transplantation. Diabetes 2003;52:2279–2286. [PubMed: 12941767]
19. Hai T, Wolfgang CD, Marsee DK, Allen AE, Sivaprasad U. ATF3 and stress responses. Gene Expression 1999;7:321–335. [PubMed: 10440233]

20. Hai T, Hartman MG. The molecular biology and nomenclature of the ATF/CREB family of transcription factors: ATF proteins and homeostasis. Gene 2001;273:1–11. [PubMed: 11483355]
21. Hai, T. The ATF transcription factors in cellular adaptive responses. In: Ma, J., editor. Gene expression and regulation. China and New York, USA: Higher Education Press and Springer, Beijing; 2006. p. 322-333.
22. Hartman MG, Lu D, Kim ML, et al. Role for activating transcription factor 3 in stress-induced beta-cell apoptosis. Mol. Cell. Biol 2004;24:5721–5732. [PubMed: 15199129]
23. Li D, Yin X, Zmuda EJ, et al. The repression of IRS2 gene by ATF3, a stress-inducible gene, contributes to pancreatic β-cell apoptosis. Diabetes 2007;57:635–644. [PubMed: 18057093]
24. Huang DR, Wang J, Kivisakk P, Rollins BJ, Ransohoff RM. Absence of monocyte chemoattractant protein 1 in mice leads to decreased local macrophage recruitment and antigen-specific T helper cell type 1 immune response in experimental autoimmune encephalomyelitis. J. Exp. Med 2001;193:713–726. [PubMed: 11257138]
25. Hohmeier HE, Mulder H, Chen G, Henkel-Rieger R, Prentki M, Newgard CB. Isolation of INS-1-derived cell lines with robust ATP-sensitive K+ channel-dependent and -independent glucose-stimulated insulin secretion. Diabetes 2000;49:424–430. [PubMed: 10868964]
26. Grey ST, Longo C, Shukri T, et al. Genetic engineering of a suboptimal islet graft with A20 preserves Beta cell mass and function. J. Immunol 2003;170:6250–6256. [PubMed: 12794157]
27. Garcia-Ocana A, Takane KK, Reddy VT, Lopez-Talavera J-C, Vasavada RC, Stewart AF. Adenovirus-mediated Hepatocyte Growth Factor Expression in Mouse Islets Improves Pancreatic Islet Transplant Performance and Reduces Beta Cell Death. J. Biol. Chem 2003;278:343–351. [PubMed: 12403787]
28. Lu D, Wolfgang CD, Hai T. Activating transcription factor 3, a stress-inducible gene, suppresses Ras-stimulated tumorigenesis. J. Biol. Chem 2006;281:10473–10481. [PubMed: 16469745]
29. Khuu CH, Barrozo RM, Hai T, Weinstein SL. Activating transcription factor 3 (ATF3) represses the expression of CCL4 in murine macrophages. Mol. Immunol 2007;44:1598–1605. [PubMed: 16982098]
30. Yin X, DeWille J, Hai T. A potential dichotomous role of ATF3, an adaptive-response gene, in cancer development. Oncogene 2008;27:2118–2127. [PubMed: 17952119]
31. Berman DM, Cabrera O, Kenyon NM, et al. Interference with tissue factor prolongs intrahepatic islet allograft survival in a nonhuman primate marginal mass model. Transplantation 2007;84:308–315. [PubMed: 17700154]
32. Leenen PJ, de Bruijn MF, Voerman JS, Campbell PA, van Ewijk W. Markers of mouse macrophage development detected by monoclonal antibodies. J. Immunol. Methods 1994;174:5–19. [PubMed: 8083537]
33. Fiaschi-Taesch NM, Berman DM, Sicari BM, et al. Hepatocyte growth factor enhances engraftment and function of nonhuman primate islets. Diabetes 2008;57:2745–2754. [PubMed: 18820214]
34. Contreras JL, Bilbao G, Smyth C, et al. Gene transfer of the Bcl-2 gene confers cytoprotection to isolated adult porcine pancreatic islets exposed to xenoreactive antibodies and complement. Surgery 2001;130:166–174. [PubMed: 11490345]
35. Rao P, Roccisana J, Takane KK, et al. Gene transfer of constitutively active Akt markedly improves human islet transplant outcomes in diabetic severe combined immunodeficient mice. Diabetes 2005;54:1664–1675. [PubMed: 15919787]
36. Hennige AM, Burks DJ, Ozcan U, et al. Upregulation of insulin receptor substrate-2 in pancreatic beta cells prevents diabetes. J. Clin. Invest 2003;112:1521–1532. [PubMed: 14617753]
37. Emamaullee JA, Rajotte RV, Liston P, et al. XIAP overexpression in human islets prevents early posttransplant apoptosis and reduces the islet mass needed to treat diabetes. Diabetes 2005;54:2541–2548. [PubMed: 16123341]
38. Rossi L, Migliavacca B, Pierigé F, et al. Prolonged islet allograft survival in diabetic mice upon macrophage depletion by clodronate-loaded erythrocytes. Transplantation 2008;85:648–650. [PubMed: 18347547]
39. Eizirik DL, Colli ML, Ortis F. The role of inflammation in insulitis and beta-cell loss in type 1 diabetes. Nat. Rev. Endocrinol 2009;5:219–226. [PubMed: 19352320]

40. Cnop M, Welsh N, Jonas JC, Jorns A, Lenzen S, Eizirik DL. Mechanisms of pancreatic beta-cell death in type 1 and type 2 diabetes: many differences, few similarities. Diabetes 2005;54:S97–S107. [PubMed: 16306347]

41. Gysemans C, Stoffels K, Giulietti A, et al. Prevention of primary non-function of islet xenografts in autoimmune diabetic NOD mice by anti-inflammatory agents. Diabetologia 2003;46:1115–1123. [PubMed: 12879250]

42. Gilchrist M, Thorsson V, Li B, et al. Systems biology approaches identify ATF3 as a negative regulator of Toll-like receptor 4. Nature 2006;441:173–178. [PubMed: 16688168]

43. Whitmore MM, Iparraguirre A, Kubelka L, Weninger W, Hai T, Williams BR. Negative regulation of TLR-signaling pathways by activating transcription factor-3. J. Immunol 2007;179:3622–3630. [PubMed: 17785797]

44. Thomas FT, Hutchings A, Contreras J, et al. Islet transplantation in the twenty-first century. Immunol. Res 2002;26:289–296. [PubMed: 12403366]

45. Zhang YC, Pileggi A, Agarwal A, et al. Adeno-associated virus-mediated IL-10 gene therapy inhibits diabetes recurrence in syngeneic islet cell transplantation of NOD mice. Diabetes 2003;52:708–716. [PubMed: 12606512]

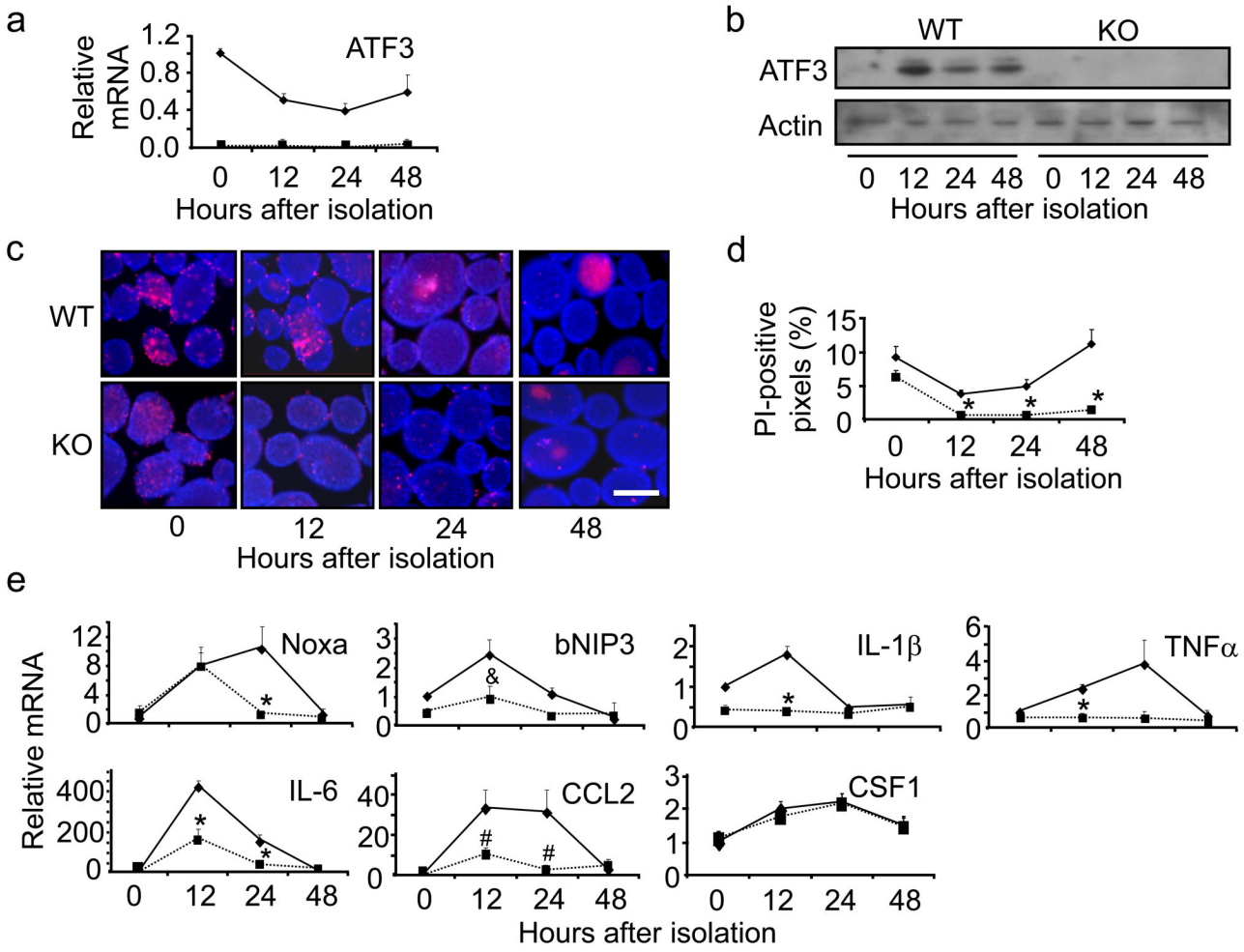

Fig. 1.

ATF3 KO islets are protected from isolation stress. **a** Primary islets from WT and *ATF3* KO mice were isolated and allowed to recover for the indicated times. *ATF3* mRNA levels were determined by qRT-PCR and standardized against β-actin. The standardized signal at time point 0 was arbitrarily defined 1. Shown are mean±SEM from three experiments. WT: solid line; KO: dotted line. **b** Same as (**a**) but immunoblot is shown (a representative of three experiments). **c** Islet cell death was evaluated by propidium iodide (red) and Hoechst (blue) stain. Groups of 100–150 islets from each group were analyzed and representative fields from each time point are shown. Bar = 400 μm. **d** Quantitation of images in (**c**). Y axis is the percentage of Hoechst positive pixels that are also PI-positive (see Supplemental Fig. 1 for detailed steps of image analysis). WT: solid line; KO: dotted line. * $p<0.001$ versus WT. **e** Same as in (**a**) except the indicated mRNAs were analyzed. Shown are representative graphs from three experiments. WT: solid lines; KO: dotted lines. * $p<0.05$, & $p=0.13$, # $p=0.08$ versus WT.

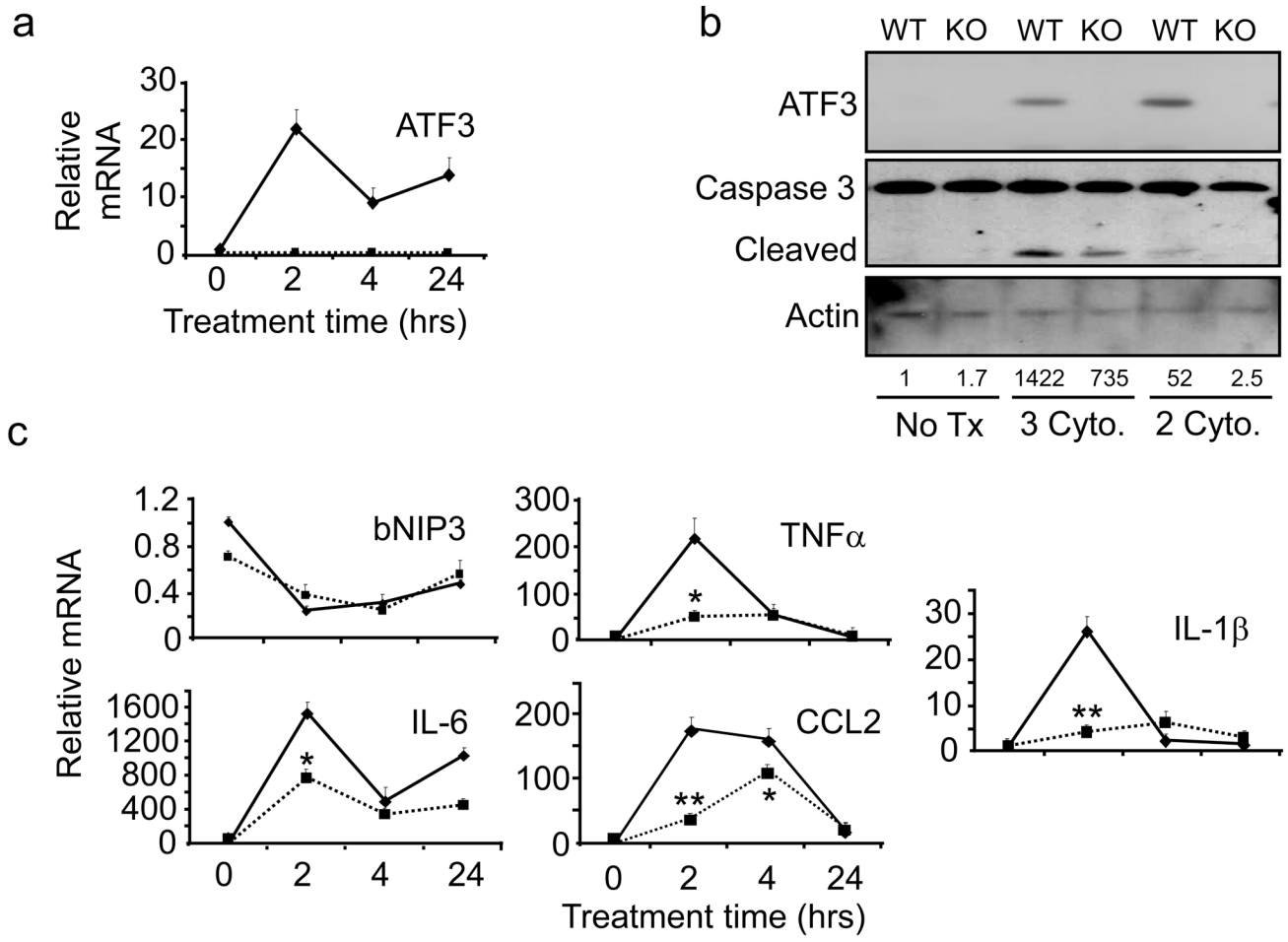

Fig. 2.

ATF3 KO islets are protected from inflammatory cytokines. **a** Primary islets from WT and *ATF3* KO mice were isolated and allowed to recover for 72 hours prior to three cytokine treatment (IL-1β, TNFα, and IFNγ). *ATF3* mRNA levels were determined by qRT-PCR and analyzed as in Fig. 1a. Shown are mean±SEM from three experiments. WT: solid line; KO: dotted line. **b** Islets prepared as in (**a**) were treated (Tx) with three cytokines (3 Cyto.) or two cytokines (2 Cyto. IL-1β and TNFα) and analyzed by immunoblot for the indicated proteins at 24 hours after treatment. Shown is a representative of three experiments. The densitometry signals for cleaved caspase 3 were standardized against that for actin; the standardized signal for WT islets with no treatment was arbitrarily defined as 1 and the relative signals are indicated at the bottom of the blot. **c** Same as in (**a**) except the indicated mRNAs were analyzed. Shown are representative graphs from four experiments. WT: solid lines; KO: dotted lines. * $p<0.05$, ** $p<0.02$ versus WT.

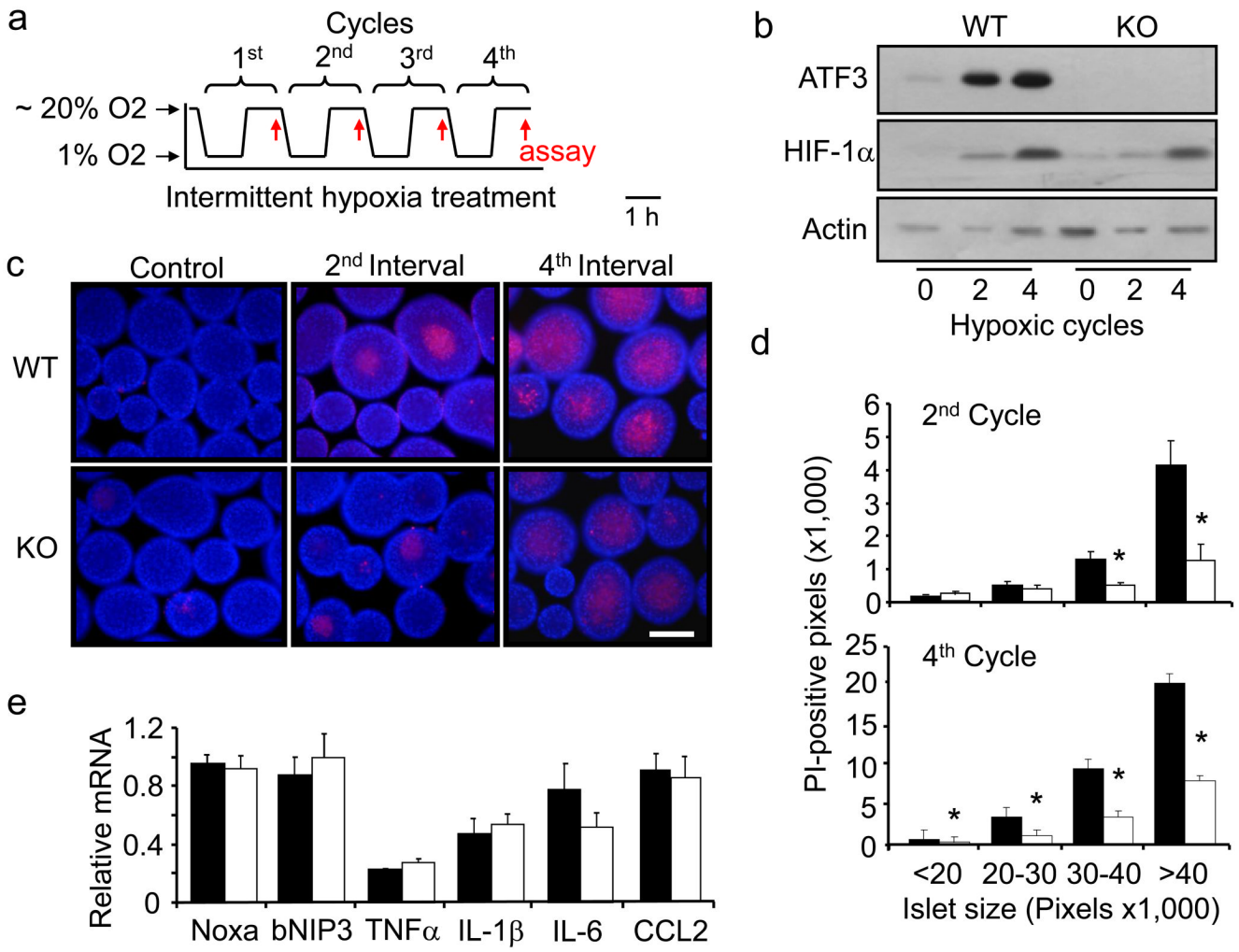

Fig. 3.

ATF3 KO islets are protected from hypoxic stress. **a** A schematic of the intermittent hypoxia treatments: hypoxia (1% O2) and normoxia (20% O2) for 1 hour each with assays at the end of each cycle (red arrows). **b** Primary islets from WT and *ATF3* KO mice were isolated and allowed to recover for 72 hours prior to hypoxia treatments. At the indicated cycles of treatments, the islets were analyzed by immunoblot for the indicated proteins. Shown is a representative of three experiments. **c** Islet cell death was evaluated by PI (red) and Hoechst (blue) stain as in Fig. 1c, except that 250–300 islets were used in each group. Shown are representative fields from the indicated cycles. Bar = 200 μm. **d** Quantitation of data in (**c**) for islets treated with two (top) or four (bottom) cycles of hypoxia. Islets were arbitrarily divided into four size groups and the percentage of PI-positive pixels (mean ±SEM) in each group are shown. WT: solid bars; KO: open bars. * $p<0.001$ versus WT. **e** Islets treated with two cycles of hypoxia were analyzed for the indicated mRNAs as in Fig. 1e. The respective mRNA level under the un-stressed condition was arbitrarily defined as 1. Shown are average values from three experiments. WT: solid bars; KO: open bars.

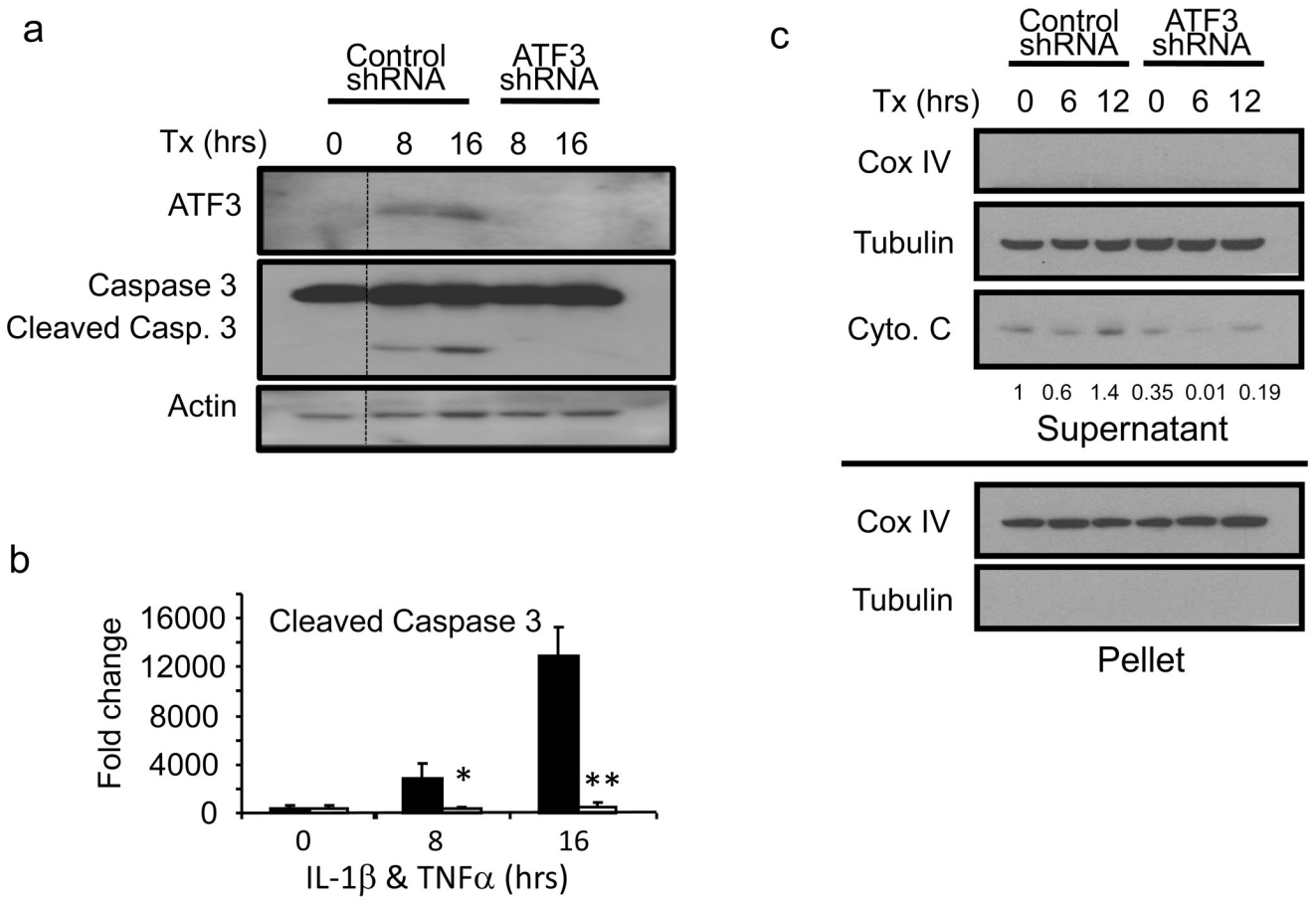

Fig. 4.

ATF3 knockdown protects beta cells from cytokine-induced caspase activation and cytochrome c release. **a** INS-r3 cells were infected with adenovirus expressing control or ATF3 shRNA for 24 hours and treated (Tx) with cytokines (IL-1β and TNFα) for the indicated hours (hrs). Total cell lysates were analyzed for the indicated proteins. A representative of three experiments is shown. **b** Blots from three experiments were quantified by densitometry. The signals for cleaved caspase 3 were standardized against that for actin and the standardized signal for control knockdown at 0 hrs was arbitrarily defined as 1. Means±SEM are shown. Control shRNA: solid bars; ATF3 shRNA: open bars. * $p<0.012$; ** $p<0.002$. **c** INS-r3 cells with control or ATF3 knockdown were treated (Tx) with cytokines as in **(a)** for the indicated hours (hrs). Cytosolic faction (supernatant) was separated from the nuclear/mitochondrial fraction (pellet), and analyzed for the indicated proteins. Cyto. c: cytochrome c; Cox IV: subunit IV of cytochrome c oxidase as a control for the pellet; Tubulin: a control for the supernatant. The densitometry signals for Cyto. c were standardized against that for tubulin. The standardized signal for control knockdown at 0 hrs was arbitrarily defined as 1 and the relative signals are indicated at the bottom of the blot.

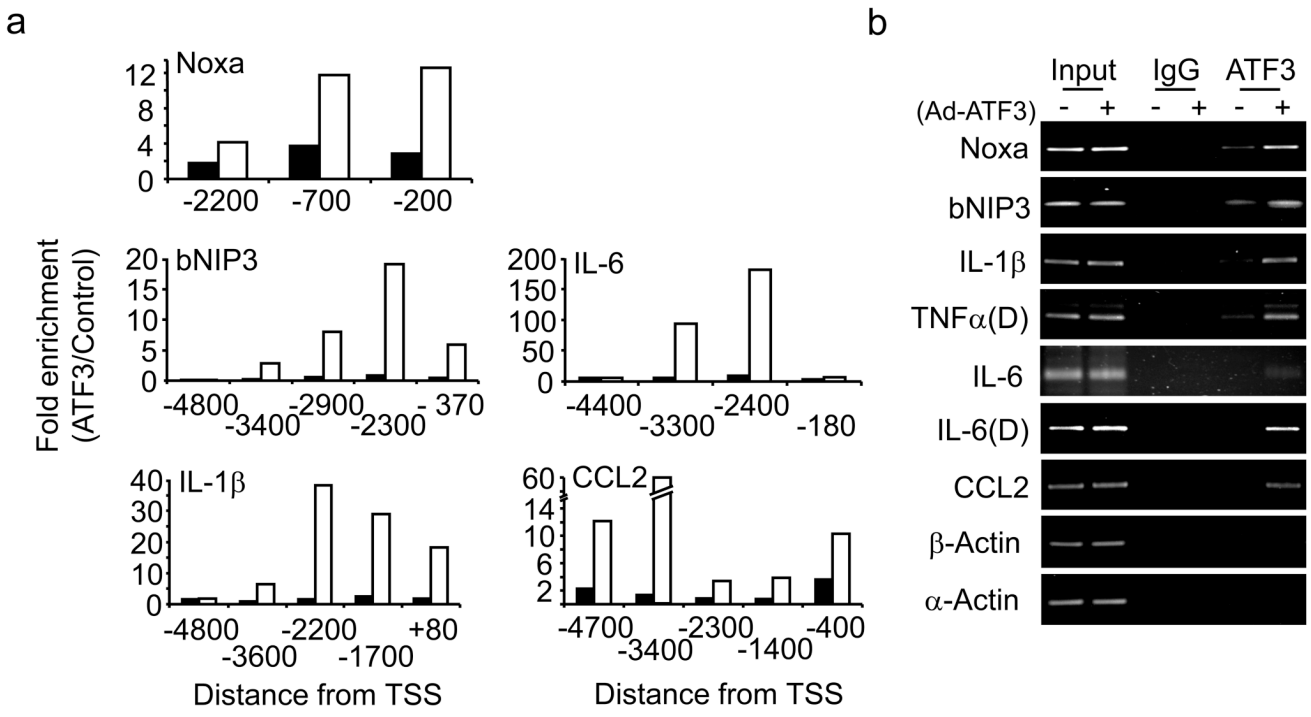

Fig. 5.

Ectopically expressed ATF3 binds to the promoters of the pro-apoptotic and pro-inflammatory target genes. **a** INS-1 cells were infected with adenovirus expressing ATF3 (Ad-ATF3) or βGal (Ad-βGal) for 24 hours prior to ChIP analysis using primer pairs (schematics in Supplemental Fig. 2) for the potential binding sites at the indicated distance from the transcriptional start site (TSS). For each primer pair, the ChIP signals were determined by qPCR and normalized to input chromatin. The normalized ChIP signals from the Ad-ATF3-infected cells were divided by that from the Ad-βGal-infected cells to obtain the "fold enrichment." Fold enrichment from immunoprecipitation using either IgG (solid bars) or ATF3 antibodies (open bars) is shown. In four independent experiments, the pattern of binding (relative ATF3 recruitment to different sites on a given promoter) was largely the same, although the absolute fold enrichment varied to some extent from one experiment to another. A representative result is shown. **b** ChIP signals were analyzed by agarose gel electrophoresis at the end of the linear phase of PCR reactions. The most proximal site for each promoter relative to the corresponding TSS was examined, except those indicated as distal (D). *TNF*α (D): −4800bp; *IL-6*(D): −2400 bp. Shown is a representative of four experiments.

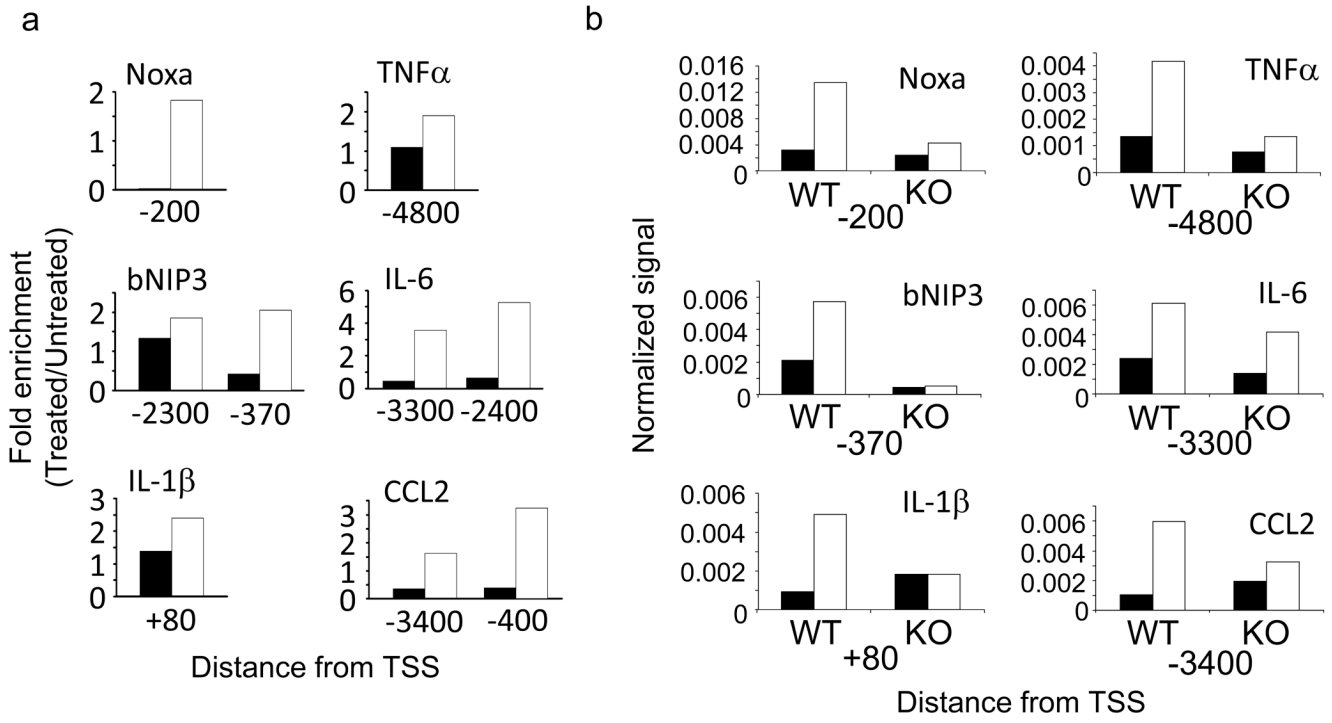

Fig. 6.

Endogenous ATF3 binds to the promoters of the pro-apoptotic and pro-inflammatory target genes. **a** INS-r3 beta cells were untreated or treated with cytokines (IL-1β, TNFα, and IFNγ), and ATF3 binding to the indicated promoters at five hours after treatment was analyzed by ChIP using the primers for the indicated sites. The normalized ChIP signals (against the input chromatin) from the treated cells were divided by that from the untreated cells to obtain the "fold enrichment." Fold enrichment from immunoprecipitation using either IgG (solid bars) or ATF3 antibodies (open bars) is shown. The experiments were carried out twice and the results from one experiment are shown. **b** WT or ATF3 KO islets immediately after isolation were treated with cytokines, and ATF3 binding to the indicated promoters at 12 hours after treatment was analyzed by ChIP. The experiments were carried out twice and the results from one experiment are shown. IgG: solid bars; ATF3 antibody: open bars.

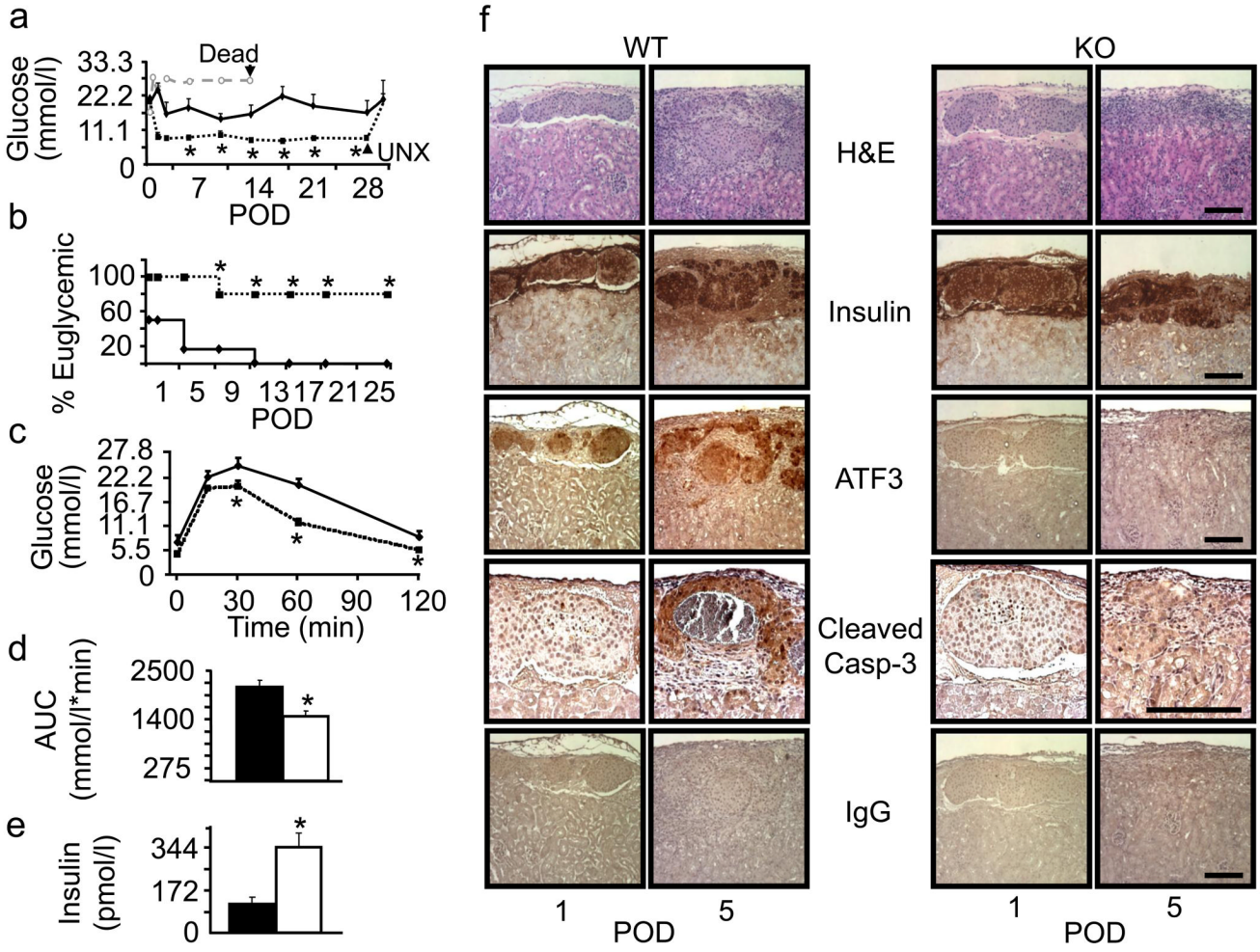

Fig. 7.

ATF3 KO islets are protected from syngeneic transplantation stress. **a** C57BL/6 mice were rendered diabetic by streptozotocin prior to receiving a marginal dose of 250 WT or *ATF3* KO islets. Non-fasted blood glucose levels were monitored from post-operative day (POD) 1 to POD28, when the grafts were removed (UNX). WT: solid line; KO: dotted line; Mock: grey dotted line. n=6 for WT and n=5 for KO islet recipients (* $p<0.05$ versus WT). A mock transplant recipient (injected with PBS) died at POD 14 as indicated. **b** Percent of mice maintaining euglycemia (blood glucose <11 mmol/l) through POD25 is shown. WT: solid line; KO: dotted line. * $p<0.05$ versus WT (Fisher's exact test). **c** The result from intraperitoneal glucose tolerance test on POD28 is shown. WT: solid line; KO: dotted line. * $p<0.05$ versus WT. **d** Area under curve (AUC) from panel **c** is shown. WT: solid bar; KO: open bar. * $p<0.005$ versus WT. **e** Fasting serum insulin on POD28 is shown. WT: solid bar; KO: open bar. * $p<0.05$ versus WT. **f** Islets grafts at the indicated PODs were analyzed by H&E stain or immunohistochemistry using the indicated antibodies. Bar=100μm.

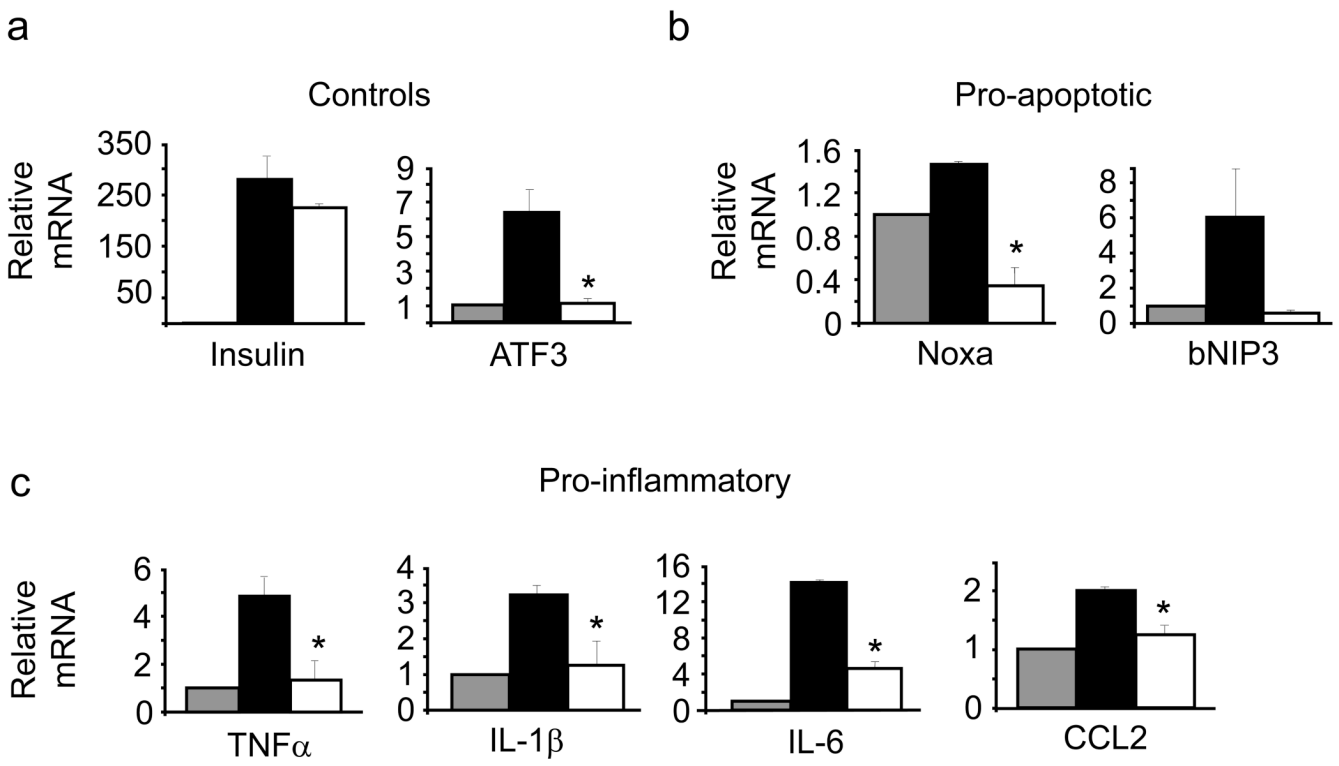

Fig. 8.

The *ATF3* KO islet grafts have reduced expression of pro-apoptotic and pro-inflammatory genes. WT and *ATF3* KO grafts derived from 400 transplanted islets were recovered on POD2 and analyzed for the indicated control (**a**), pro-apoptotic (**b**), or pro-inflammatory (**c**) genes by qRT-PCR and standardized against β-*actin*. The standardized signal from mock transplant (injected with PBS) was arbitrarily defined as 1. Insulin mRNA was used as a quality control for the grafts. WT: solid bars; KO: open bars; Mock transplant: grey bars. * $p<0.05$ versus WT.

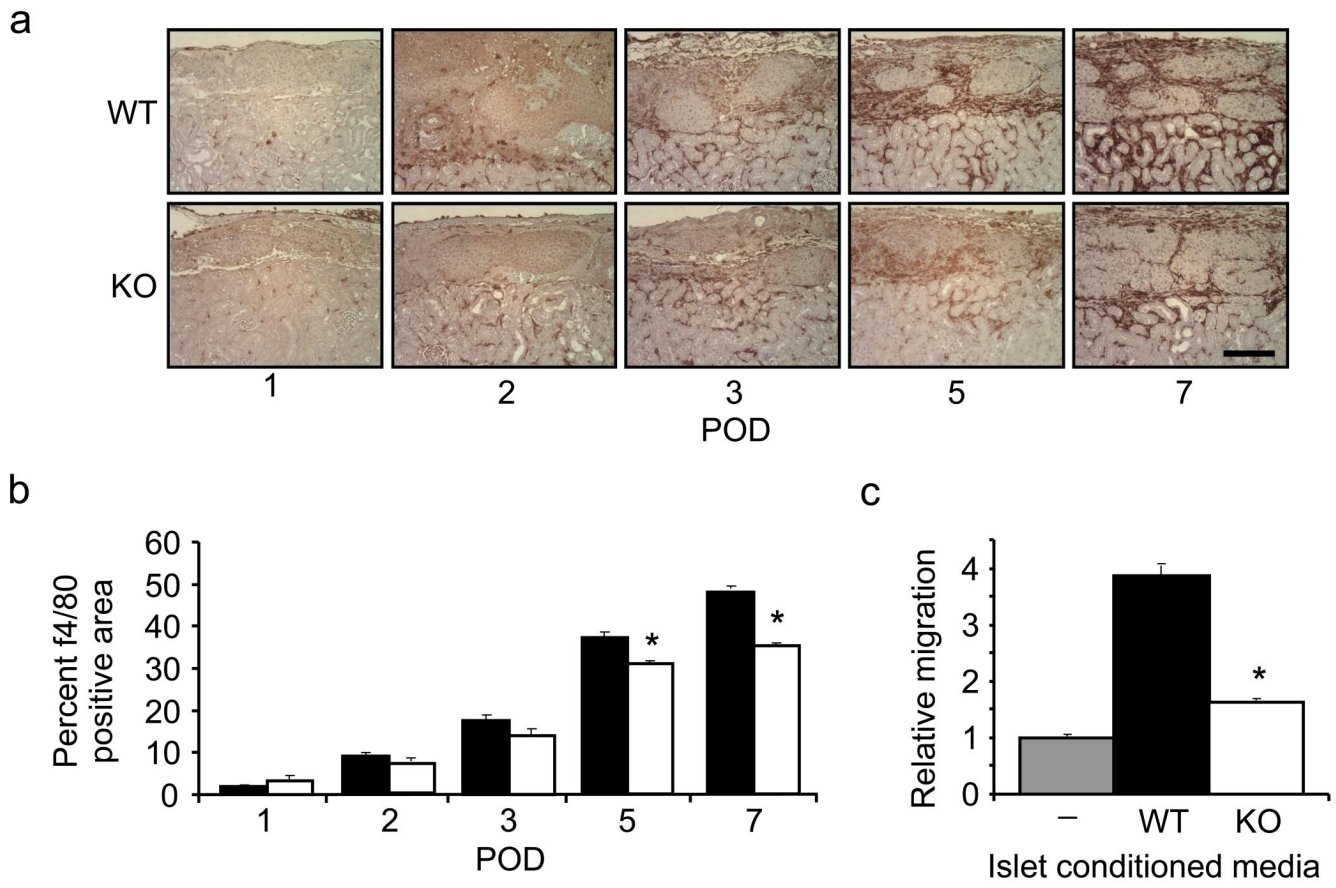

Fig. 9.

Transplanted ATF3 KO islets promote less macrophage recruitment. **a** WT and ATF3 KO grafts at the indicated PODs were analyzed by immunohistochemistry for F4/80, a macrophage marker. Shown are representative fields from 4 mice each with 10–20 fields examined in each mouse. Bar=100μm. **b** Immunohistochemistry data in panel **a** were quantified using the methods detailed in the text and Supplemental Fig. 4. WT: solid bars; KO: open bars. * $p<0.05$ versus WT. **c** Bone marrow derived macrophages were analyzed by the Boyden chamber migration assay using either media control (−) or conditioned media from the indicated islets in the bottom chambers. Migrated cells were stained by crystal violet and the signal from the media control (grey bar) was arbitrarily defined as 1. The signals from the islet conditioned media were then standardized against the total RNA contents in the islets. *$p<0.05$ versus WT.